Marine Geology 405 (2018) 12–22

Contents lists available at ScienceDirect

Marine Geology

journal homepage: www.elsevier.com/locate/margo

Rip current circulation and surf zone retention on a double barred beach

Shari L. Gallop[a,*], Karin R. Bryan[b], Sebastian J. Pitman[c], Roshanka Ranasinghe[d,e,f], Dean R. Sandwell[b], Shawn R. Harrison[g]

[a] Department of Environmental Sciences & Macquarie University Marine Research Centre, 12 Wally's Walk, Macquarie University, NSW 2109, Australia
[b] School of Science, University of Waikato, Private Bag 3105, Hamilton, New Zealand
[c] Department of Geography, University of Canterbury, Private Bag 4800, Christchurch 8140, New Zealand
[d] Department of Water Science and Engineering, IHE Delft Institute for Water Education, PO Box 3015, 2601 DA, Delft, the Netherlands
[e] Water Engineering and Management, Faculty of Engineering Technology, University of Twente, PO Box 217, 7500 AE, Enschede, the Netherlands
[f] Harbour, Coastal and Ocean Engineering, Deltares, PO Box 177, 2600 MH Delft, the Netherlands
[g] Pacific Coastal and Marine Science Center, U.S. Geological Survey, 2885 Mission Street, Santa Cruz, CA 95060, USA

ARTICLE INFO

Editor: E Anthony

Keywords:
Beach processes
Rip currents
Rip channels
Surf zone exchange
Beach hazards
Coastal morphodynamics

ABSTRACT

Rip currents have an important control on the exchange of water and advected materials such as sediment and pollutants, between the surf zone and inner shelf. Concurrent in situ Eulerian and Lagrangian (GPS drifter) data of surf zone waves and currents were combined with video data on wave breaking patterns over the inner and outer bars on a high energy, double-barred beach. The data collectively show how the occurrence of wave breaking over the outer bar changes the behavior of a channel rip current, and the exchange process. On both days, there was a prominent clockwise eddy in the surf zone, for which the seaward-heading portion formed a rip current in a well-defined channel rip, incised into the inner bar. Exit rate (measured with drifters) from the surf zone to inner shelf decreased significantly with increased wave breaking over the outer bar, from 71% exits to 6% over the two days. Exit rate appears to be driven by the balance between wave breaking over the inner and outer bars and pulsing of currents within the surf zone. Under higher wave conditions, there were stronger pulsations in surf zone currents and more surf zone exits. However, higher wave conditions caused wave breaking over the outer bar. This breaking increases vorticity around the outside of the surf zone eddy, which increases surf zone retention. This is in contrast to previous studies showing that vorticity is highest at the center of surf zone eddies. Under such conditions, drifter exits were rare, and occurred due to vortex shedding. During lower incident wave conditions, eddy vorticity was lower, and drifters could relatively freely exit the surf zone. This is one of the few studies that investigate surf zone circulation on a high energy, double-barred beach.

1. Introduction

On surf beaches, water is exchanged between the surf zone and inner continental shelf (Smith and Largier, 1995; Brown et al., 2009; Spydell et al., 2014; Hally-Rosendahl et al., 2015; Suanda and Feddersen, 2015), and also transports sediment (Holman et al., 2006; Loureiro et al., 2012; Thorpe et al., 2013; Spydell, 2016), nutrients (Castelle et al., 2010a), diatoms (Talbot and Bate, 1987), larvae (Defeo and McLachlan, 2005; Fujimura et al., 2014; Spydell, 2016), pathogens (Feng et al., 2013; Hally-Rosendahl et al., 2015) and other pollutants (Spydell et al., 2007, Spydell and Feddersen, 2012, Spydell, 2016) in nearshore and shelf waters (Kumar and Feddersen, 2016a, 2016b). However, the exchange process is highly variable in space and time (Suanda and Feddersen, 2015), and understanding the mechanisms remains a challenge.

Surf zone exchange occurs on all types of wave-dominated beaches (e.g., Spydell et al., 2007, 2014; Spydell and Feddersen, 2009, 2012; Feddersen et al., 2011; Suanda and Feddersen, 2015). On beaches with sand bars, a key conduit for this exchange is rip currents (rips) (Kumar and Feddersen, 2016a, 2016b). Rips are narrow, seaward-directed flows that extend from close to the shoreline, through the surf zone and sometimes beyond (Short, 1985; Aagaard et al., 1997; Castelle et al., 2016a, 2016b). There are three broad categories of rip currents, which can be subdivided into six fundamental types (Castelle et al., 2016a, 2016b). *Hydrodynamically-controlled rips* (sometimes called *transient rips*) occur on beaches that have uniform bathymetry alongshore and are transient in space and time (Johnson and Pattiaratchi, 2004, 2006; Castelle et al., 2014a; Feddersen, 2014; Suanda and Feddersen, 2015).

* Corresponding author.
E-mail address: shari.gallop@mq.edu.au (S.L. Gallop).

https://doi.org/10.1016/j.margeo.2018.07.015
Received 6 June 2018; Accepted 31 July 2018
Available online 02 August 2018
0025-3227/ © 2018 Elsevier B.V. All rights reserved.

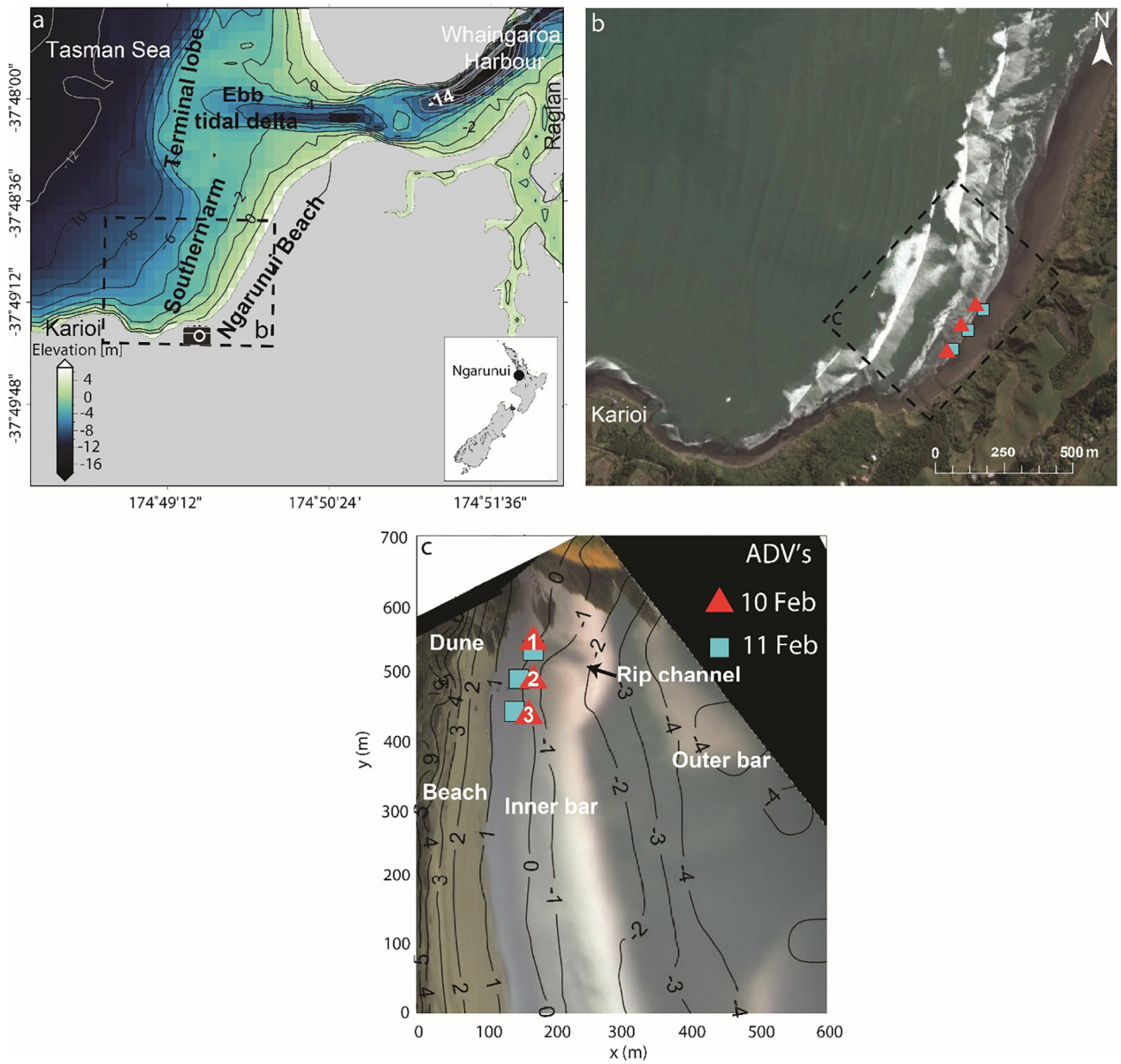

Fig. 1. (a) Study site location and bathymetry (compiled by Harrison and Hunt, 2014, with data sources detailed in Harrison, 2015), indicating the location of the Cam-Era camera (camera symbol). (b) Google Earth image from 22/07/2015 of the study area in the box indicated in (a). (c) timex Cam-Era image of the focus area on 11/02/2015 at 09:30 shown in (b), where black areas are outside the camera field of view. Bathymetry contours in (b) were collected on 5 February 2015 with RTK GPS down to low tide level and merged with bathymetry from Harrison and Hunt (2014), with a vertical datum of mean sea level. Coordinates in (c) and throughout the rest of the paper are local and in m, with an arbitrary zero, and rotated 153° relative to true north to align with the shoreline. Locations of the Acoustic Doppler Velocimeters (ADVs) on each day are indicated by the numbered symbols, also shown in (b) for reference.

The two types of *hydrodynamically-controlled rips* are *shear instability rips* which can form due to shear instabilities of longshore currents (Özkan-Haller and Kirby, 1999; Spydell et al., 2009; Castelle et al., 2014a; Feddersen, 2014), and *flash rips*, which are episodic bursts of water that jets offshore, due to transient surf zone eddies (Spydell and Feddersen, 2009; Feddersen, 2014). *Bathymetrically-controlled rips* are forced by alongshore variability in hydrodynamics, driven by bathymetric variations. These rips can be subdivided into *channel rips*, which occupy channels in between sand bars (Holman et al., 2006; Gallop et al., 2009; Dalrymple et al., 2011), and *focused rips* which form due to variations in offshore bathymetry (Long and Özkan-Haller, 2005, 2016). *Boundary-controlled rips* occur along lateral boundaries such as headlands (Gallop et al., 2011; McCarroll et al., 2014), piers and groynes (Pattiaratchi et al., 2009; Scott et al., 2016), and can be divided into *shadow rips*, which form against a boundary in the area shadowed from incident waves (Gourlay, 1974; Castelle and Coco, 2012), and *deflection rips* which form due to strong alongshore currents generated by incoming waves, that are deflected against a lateral boundary (Dalrymple et al., 2011; Scott et al., 2016). This paper focuses on surf zone exchange on a beach with *channel rips*, that is, rip currents located within channels in between sand bars, driven by alongshore variation in breaking wave energy dissipation, due to the alongshore variability in water depth (Bowen et al., 1968).

Surf zone exchange can be measured in terms of retention and exit rate of material from the surf zone (MacMahan et al., 2010; Reniers et al., 2010; Castelle et al., 2014b; Suanda and Feddersen, 2015). An exit occurs when currents move water and material seaward of the wave breaker zone onto the inner shelf, as opposed to retention by

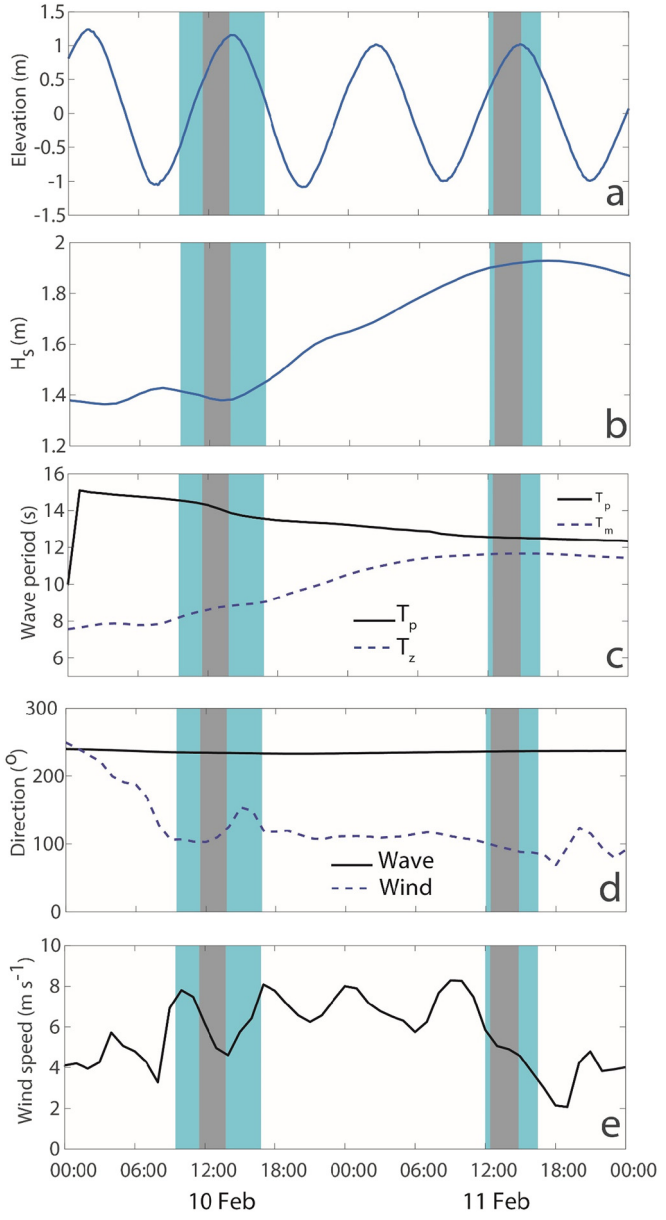

Fig. 2. (a) Water level measured at Raglan Wharf in 2015; and offshore wave conditions from NZLAM_12 and nzwave_12 respectively, including: (b) H_s; (c) T_z and T_p; (d) mean wave and wind direction (from); and (e) wind speed. The duration of the ADV deployments is highlighted by the blue segments (lighter color) and drifter deployments by grey segments (darker color). (For interpretation of the references to color in this figure legend, the reader is referred to the web version of this article.)

recirculation back into the surf zone by surf zone eddies (Austin et al., 2010). Exit rate is defined here as the rate of exits per rip entry (after MacMahan et al., 2010; McCarroll et al., 2014; Scott et al., 2014; Pitman et al., 2016). Exit rate is a critical measure of the hazard to swimmers from rip currents, which depends not only on the current speed, but also on the circulation pattern (McCarroll et al., 2013; Scott et al., 2014); whether a rip current circulates within a surf zone eddy or exits through the breaker zone may also determine the best escape strategy (MacMahan et al., 2010; Miloshis and Stephenson, 2011; McCarroll et al., 2013), so is central to beach safety education (Brander and Macmahan, 2011; Kumar and Feddersen, 2016a, 2016b; Van Leeuwen et al., 2016).

Surf zone exits from eddies are driven by pulsations in rip current velocity. Pulsations of surf zone currents can occur at infragravity frequencies (~25–300 s), which can be caused by standing infragravity waves (Sonu, 1972; MacMahan et al., 2004a), and wave groups (Spydell and Feddersen, 2009; Reniers et al., 2010; Feddersen, 2014). In addition, recent research has revealed the presence of vortical motions at Very Low Frequencies (VLF) (4–10 min) (MacMahan et al., 2004b; Reniers et al., 2010; Feddersen et al., 2011; Castelle et al., 2013, 2014b; Houser et al., 2013; Brown et al., 2015), which may be forced by spatially-varying wave groups (Reniers et al., 2007; Castelle et al., 2013). Stokes drift also has an important influence on exit rate, by reducing offshore current velocities (Reniers et al., 2009) and inducing a return Eulerian circulation (Kumar and Feddersen, 2016a, 2016b).

Research on rip currents at high energy wave-dominated beaches is sparse, (Brander and Short, 2000), despite such beaches having the highest hazard rating in the Handbook of Drowning (Bierens, 2006). Such beaches in micro- to meso-tidal ranges often have multiple sand bars (Masselink and Short, 1993; Short and Aagaard, 1993; Castelle et al., 2010c, 2014b). Here, the inner bar and surf zone can develop unique morphology and circulation that does not occur on single-barred beaches (Castelle et al., 2010b, 2014b; Price et al., 2014), and the alongshore-variable bathymetry can further complicate mixing. This is because in addition to horizontal mixing by rotational flows that also occurs on alongshore-uniform beaches without sand bars, mean circulation features can also contribute (Brown et al., 2009). The aim of this study was to investigate surf zone exchange on a double barred beach, including how wave breaking over inner and outer bars controls rip circulation. This was explored in a channel rip current over two consecutive days, where variations in wave height controlled the occurrence of wave breaking over the outer bar. A combination of data were used, including in situ Eulerian and Lagrangian (drifter) data of surf zone waves and currents, and video data of wave breaking patterns over the inner and outer bars.

2. Materials and methods

2.1. Study site

Ngarunui Beach is located on the west coast of the North Island of New Zealand, near the township of Raglan (Fig. 1a). Ngarunui is a double barred, 2 km-long high energy beach, with a tidal inlet to the north, and a volcanic headland (Karioi) to the south (Fig. 1a and b). The beach consists of titanomagnetite sand (Sherwood and Nelson, 1979) with D_{50} between 200 and 400 μm (Huisman et al., 2011; Guedes et al., 2013) and has a gentle slope with β_{mean} of 0.014 over the intertidal region (Guedes et al., 2013). Tides are semidiurnal with typical neap and spring ranges of 1.8 and 2.8 m respectively (Walters et al., 2001). Average offshore significant wave height (H_{so}) is 2 m and mean spectral period (T_z) is 7 s (Gorman et al., 2003). The dominant wave direction is southwesterly (Sherwood and Nelson, 1979; Gorman et al., 2003), thus Karioi generally partially shelters the beach (Harrison, 2015). Ngarunui Beach is a popular beach for surfers and swimmers and has had recent fatalities despite lifeguards at the southern end.

The study area was at the southern end of the beach, well away from the harbour inlet. The focus was on a channel rip current incised into the inner bar (Fig. 1c). This channel is ~300 m away from the headland, although it appears closer in Cam-Era images such as Fig. 1c due to shadowing of the field of view by cliff overhang. This rip channel had a prominent surf zone on either side, thus is a channel rip current, not a boundary-controlled rip (as described in Castelle et al., 2016a, 2016b). The outer bar (Fig. 1c) forms a continuation of the southern arm of the terminal lobe of the ebb tidal delta, located at the inlet to Whaingaroa Harbour (Harrison, 2015). This arm moves periodically offshore during large swell events, and migrates shoreward during smaller swell events that typically occur in summer (Harrison et al., 2017). The depth at which wave breaking occurs varies greatly, with tide and wave conditions determining whether waves break over the terminal lobe, outer, and/or inner bar (Guedes et al., 2013).

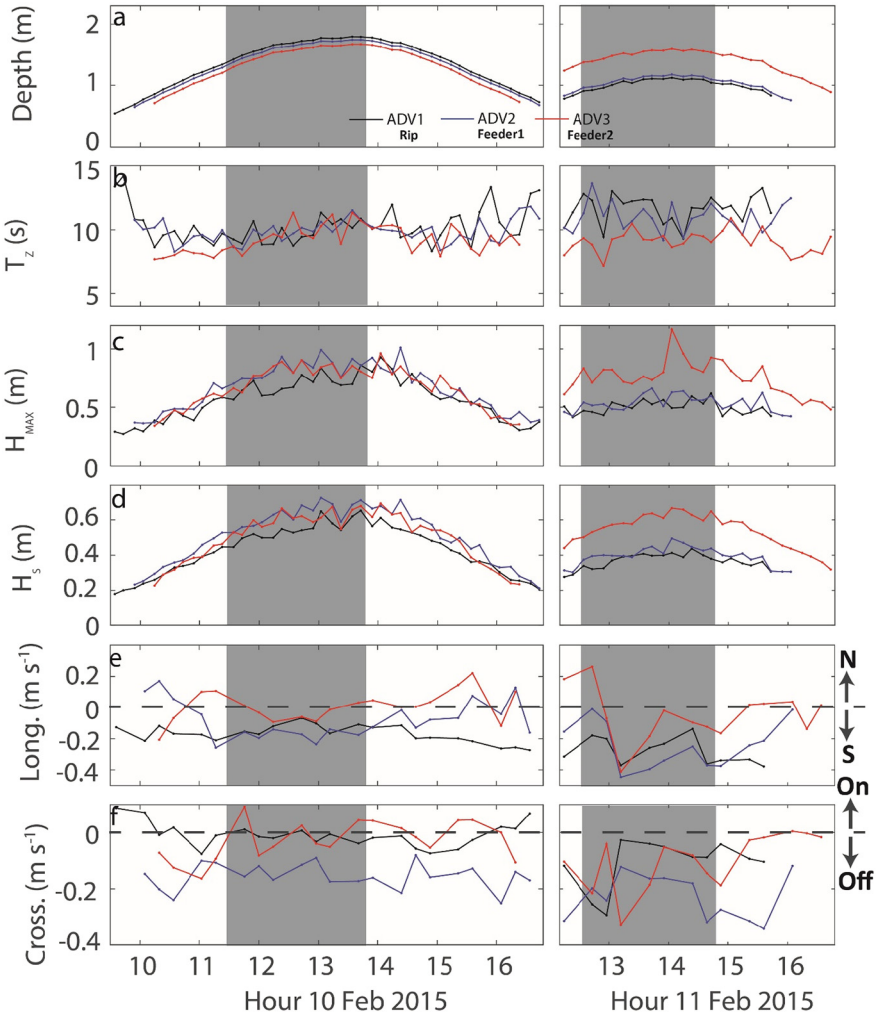

Fig. 3. Sea level and wave parameters for each ADV averaged for 2048 measurements (~8.5 min): (a) water depth to the sea bed; (b) T_z; (c) H_{max}; (d) H_s; and currents averaged for each ~17 min burst in the (e) longshore; and (f) cross-shore. Grey shaded areas show drifter deployment times; and arrows combined with dashes lines on right hand side of (e) and (f) show is currents are heading north (N) or south (S) alongshore; and onshore (On) or offshore (Off). (For interpretation of the references to color in this figure legend, the reader is referred to the web version of this article.)

Table 1
Mean hydrodynamic conditions during drifter deployments.

Date in 2015	Water level (m)	Offshore H_{so} (m)	Offshore T_{zo} (s)	Offshore T_{po} (s)	Nearshore H_s (m)	Nearshore T_z (s)
10 Feb	0.88	1.4	8.7	14.2	0.60	9.9
11 Feb	0.83	1.9	11.7	12.5	0.47	10

2.2. Field measurements

Field measurements were collected on 10 and 11 February 2015 (hereafter referred to as days 1 and 2 respectively), using three Triton Sontek Acoustic Doppler Velocimeters (ADVs) (Fig. 1c) and ten GPS drifters (Gallop et al., 2015, 2016). The ADVs were placed in an alongshore array, with one just shoreward of the base of the rip channel, and two in the feeder channel adjacent to the rip (Fig. 1c). They were upward-facing with the housing buried, so that the initial sensor height was 0.35–0.6 m above the bed, and collected 4096 samples at 4 Hz every 20 min. Spectral analysis was undertaken on detrended ADV current and pressure records.

The GPS drifters were based on the designs of Schmidt et al. (2003) and MacMahan et al. (2009) and were used to measure rip current velocities and exits. QStarz BT-Q100eX GPS loggers were used in the drifters, which record both position and velocity at 10 Hz, where velocity has accuracy of 0.1 m s^{-1} according to product specifications. The standard deviation for horizontal position was 3.78 m ± 1.20 m, estimated from a drifter left in a static position onsite. Drifters were deployed initially by being waded out to waist-depth at the base of the rip channel, before being released, and retrieved from the shore or using a jetski. Drifter data were quality controlled to remove periods when the instruments were dragging on the bed. Similar to previous studies (MacMahan et al., 2010; Austin et al., 2013; Scott et al., 2014; Pitman et al., 2016), drifters were retrieved for 4 reasons: because they: (1) exited the surf zone; (2) washed in towards shore and contacted the seabed; (3) travelled alongshore to outside the area of interest, within which they could be safely monitored and retrieved; and (4) 'other' reasons (e.g. retrieval from busy surfing areas, or at the end of an experiment). Position and velocity data were collected at 1 Hz. Velocity data were low-pass filtered using a Butterworth filter with a cut-off frequency of 0.05 Hz (Johnson and Pattiaratchi, 2004; McCarroll et al.,

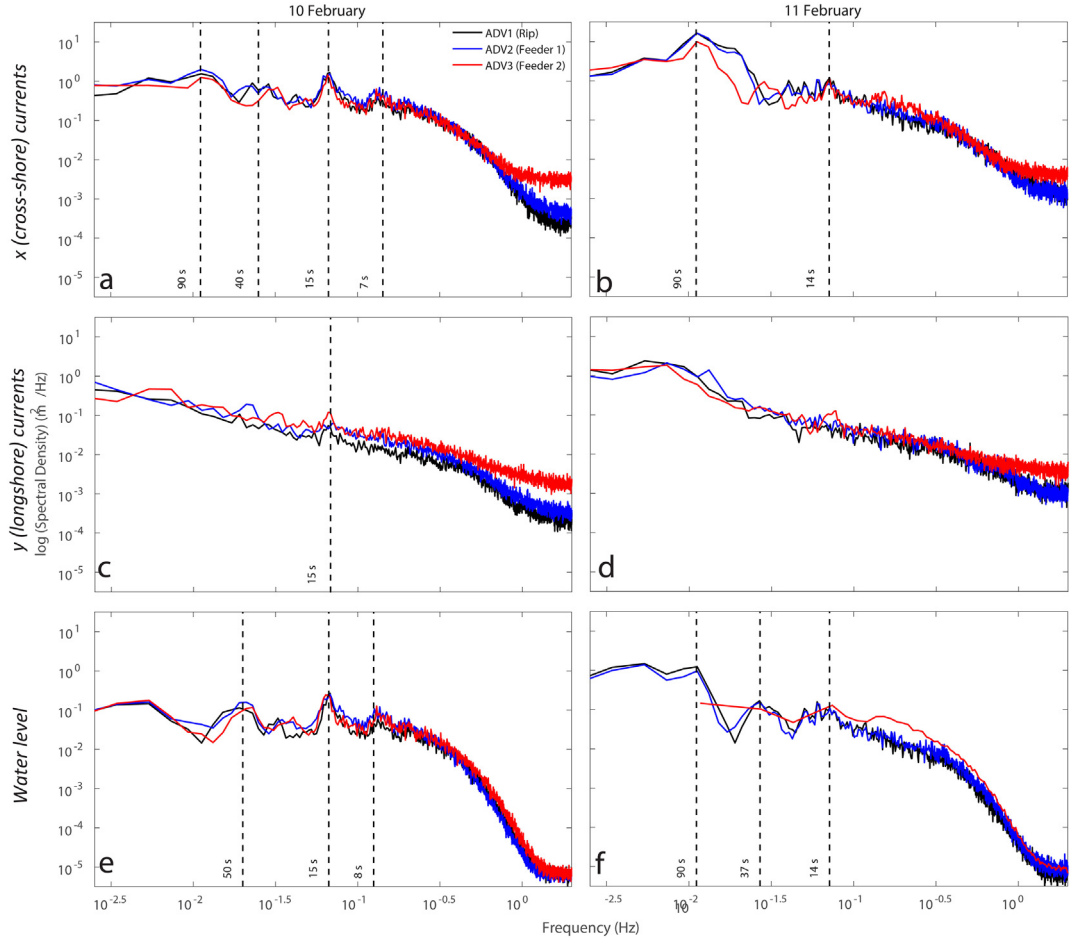

Fig. 4. Mean spectra for each frequency for ADV deployments on each day in 2015, calculated using Fast Fourier Transform with 1024 bins. Cross-shore current spectra are shown in (a) and (b); longshore in (c) and (d), and water level in (e) and (f). The periods of prominent peaks in spectral density are inidicated with dashed lines. (For interpretation of the references to color in this figure legend, the reader is referred to the web version of this article.)

2014) to average short wave-motion and other noise. A 10 m × 10 m grid was used across the surf zone to resolve the circulation patterns, as in previous studies (Austin et al., 2010; MacMahan et al., 2010; Austin et al., 2013; Scott et al., 2016; Pitman et al., 2016). Vorticity (Γ) is the change in orientation of a water parcel without change in area or shape (Molinari and Kirwan Jr., 1975), and represents local rotational motion/velocity shear (MacMahan et al., 2010). Γ is calculated here (following MacMahan et al., 2010; McCarroll et al., 2014; Pitman et al., 2016) as:

$$\Gamma = \frac{d\bar{v}}{dx} - \frac{d\bar{u}}{dy} \quad (1)$$

where u and v are velocity in x and y direction at location x, y.

The study area was observed remotely via the 'Cam-Era' video system, consisting of two cameras located at ~95 m above the beach on top of the hill at the southern end of the beach (Fig. 1a) (Harrison et al., 2017). These overlook the nearshore region, including Ngarunui Beach, the inlet to Whaingaroa Harbour and the ebb-tidal delta at its entrance. Both are Lumenera LE 375 video cameras with a 7.7 × 6.1 mm color CMOS sensor, a 2048 × 1536 array (3.1 MP) and a 25.5 mm fixed focal length lens, and have slightly overlapping fields of view which enable a broad composite view of the region (Guedes et al., 2013; Harrison, 2015; Simarro et al., 2015). In this paper, coordinates are local and given in m, with an arbitrary zero, and are rotated 153° relative to true north to align with the shoreline (Fig. 1c). Normally, 2400 image pairs care collected over 20 min at 2 Hz during daylight hours, which are averaged to create a time-exposure (timex) image. However, during the experiment the camera recorded at 1 Hz. There were camera outages on both days during part of the drifter deployments, indicated in Fig. 8. The boundary of persistent water and foam from breaking waves was digitized from rectified images as the location of wave break-point, in order to assess the influence of wave and tide conditions on the relative impact of the outer and inner sandbars to local wave breaking. While the focus here is on whether breaking occurred or not, we acknowledge that the actual position of shallow sandbars (or other bathymetric perturbations) initiating the wave breaking can differ by up to 10 m depending on offshore wave height, water level and bathymetry (Van Enckevort and Ruessink, 2001).

Bathymetry was surveyed down to low tide using RTK-GPS on 5 February 2015, and bathymetry from the wider area was compiled by Harrison and Hunt (2014) using a variety of sources including multibeam (2013) and singlebeam (2008–2009) echosounders, LiDAR (2010 – 2011), and digitized navigational charts (1961 and 1977). Water level was measured at Raglan Wharf in the main channel of Whaingaroa Harbour (Fig. 1a). Offshore wave conditions were obtained from the nzwave_12 wave forecast/hindcast, which used the WAVEWATCH v3.14 model, provided by the National Institute of Water and Atmospheric Research (NIWA). Hourly data were used from the grid cell closest to Ngarunui, (37.777843° S, 174.66760° E), in 53 m water depth. Times are given as New Zealand Daylight Time (NZDT).

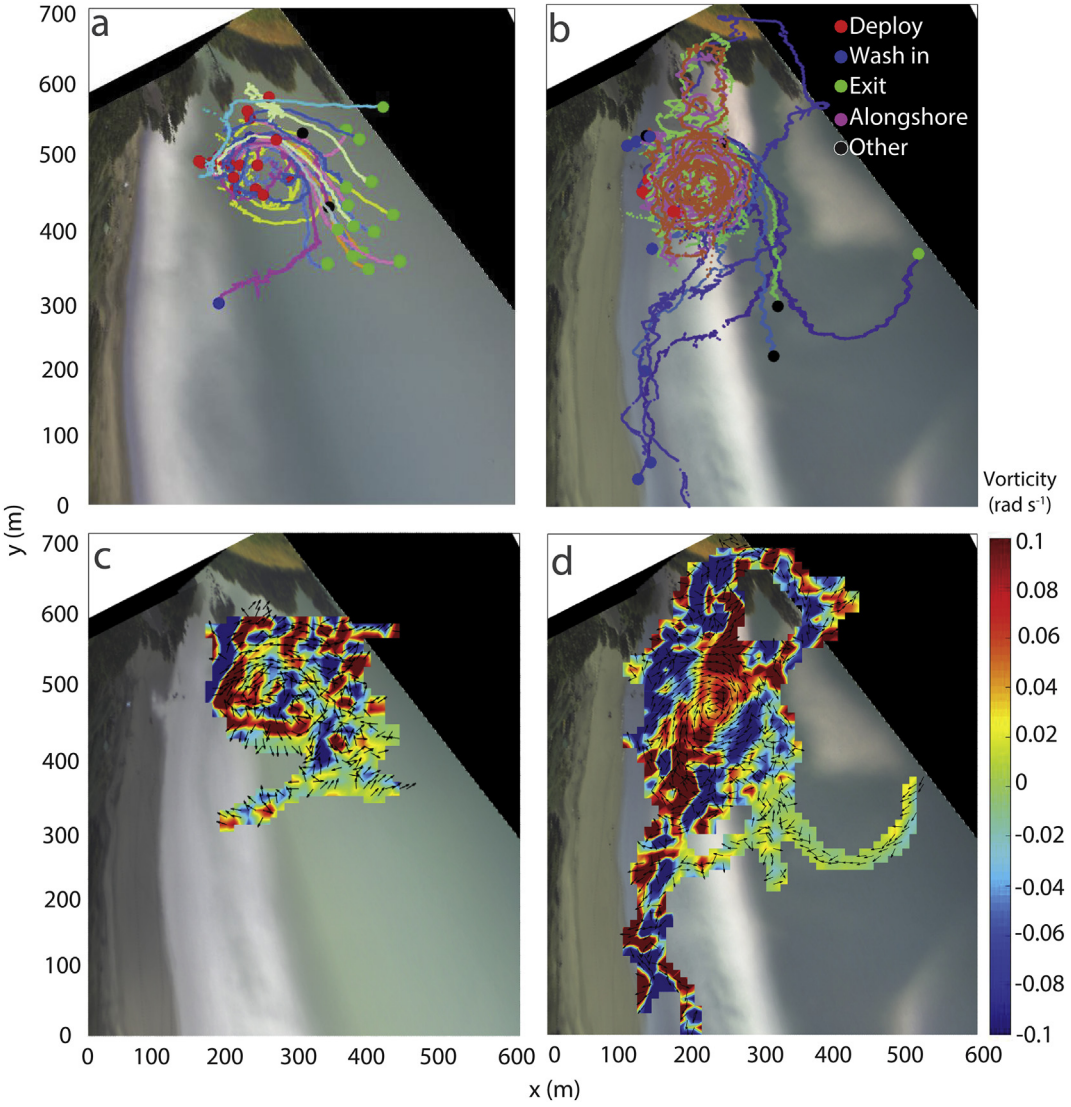

Fig. 5. Quality controlled drifter tracks on (a) day 1 (10 February) with timex image from 14:30 and (b) day 2 (11 February) with timex image from 10:30 where dots show deployment and retrieval locations. (c) and (d) show the mean vorticity (Γ) (color) and direction (arrows) in each 10 m × 10 m cell on day 1 and day 2 respectively. (For interpretation of the references to color in this figure legend, the reader is referred to the web version of this article.)

3. Results

3.1. Hydrodynamic forcing

3.1.1. Offshore wave conditions

The experiment was undertaken as tidal range decreased from a spring to a neap tide; tidal range decreased from 2.32 m on day 1, to 2.01 m on day 2 (Fig. 2a). Drifter deployments were undertaken on the rising tide on both days (Fig. 2a). Offshore wave conditions were moderate on day 1, with H_s of ~1.4 m, which increased to 1.9 m on day 2 (Fig. 2b). This 0.5 m increase in wave height doubled incident wave energy (E), estimated from Eq. (2), to be 1230 J m^{-2} on day 1, and 2270 J m^{-2} on day 2.

$$E = {}^{1}/_{16}\rho g H_{so}^{2} \quad (2)$$

where ρ is water density and and g is acceleration due to gravity. This increase in H_s was accompanied by an increase in T_z from ~9 s on day 1, to 12 s on day 2 (Fig. 2c). Peak wave period (T_p) decreased from ~14 s on day 1 to 1~2.5 s on day 2 (Fig. 2c), thus the wave field narrowed significantly in terms of period from day 1 to day 2. Swell waves were incident from WSW for the duration of the experiment, and wind was easterly on both days (Fig. 2d). Wind speed was an average of about 6.5 m s^{-1} during the day 1 deployments, and 4 m s^{-1} on day 2.

3.1.2. Nearshore waves and currents

Nearshore (depth of 1–2 m) wave height (Fig. 3c and d) was strongly tidally-modulated (Fig. 3a). On day 1 H_s and maximum wave height (H_{max}) varied from as low as 0.2 m and 0.4 m (respectively) at low tide, and reached up to 0.75 m and 1 m at high tide (Fig. 3c and d). These waves had T_z largely between 8 and 10 s (Fig. 3b). On day 2, H_s reached up to 0.4 m at ADVs 1 and 2, and up to 0.6 m at ADV3; and H_{max} was fairly constant at 0.5 m except at ADV3 where it reached > 1 m. These waves had T_z of 8–12 s. The mean hydrodynamic conditions during the daily drifter deployments are summarized in Table 1. Similar mean wave conditions and tidal modulation were observed regardless of location within the surf zone.

On both days, longshore currents measured by the ADVs headed largely in a southerly direction (indicated by negative values in Fig. 3f), i.e., towards Karioi (Fig. 1a), towards the prominent rip-current channel towards the sound (marked on Fig. 1c), near the location of ADV 1. This is consistent with the clockwise surf zone circulation cell in this area, revealed by the drifter tracks (Fig. 5c and d and detailed

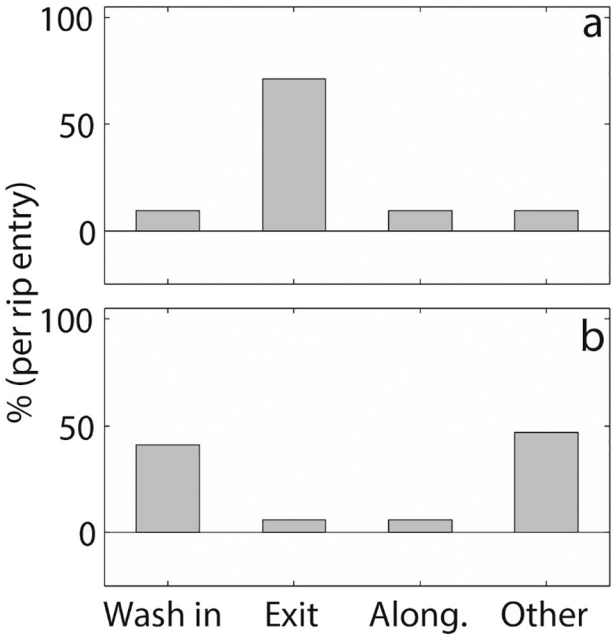

Fig. 6. Reasons for drifter retrieval on (a) day 1 (10 February) and (b) day 2 (11 February). Note that drifter tracks obscure the wave breaking patterns and rip channel shown in Fig. 1c.

below in Section 3.2). Cross-shore currents were mostly directed offshore during all ADV deployments (indicated by negative values in Fig. 3g), also consistent with the presence of the prominent rip current at the location of ADV 1, with mean velocities of ~0.3 to 0.5 m s^{-1}.

3.1.3. Current and water level spectra

ADVs were located close to shore when the drifters were deployed, thus ADV and drifter locations are not co-located. However, ADV data were still useful to investigate spectral energy in the surf zone in order to interpret drifter data. Spectral analysis shows that there was significantly higher spectral density in the cross-shore direction than longshore. For cross-shore currents, spectral density was an order of magnitude higher on day 2 (Fig. 4b) compared to day 1 (Fig. 4a). The maximum spectral density for cross-shore currents on both days was in the infragravity band at the 90s period (0.011 Hz), where this peak increased from maximum of 0.7×10^0 on day 1 to 1.6×10^1 on day 2 (Fig. 4a, b). This increase is consistent with the increase in incident wave height between these two days. On day 1, there were clear peaks at swell wave periods of 7 s (0.14 Hz) and 15 s (0.066 Hz) (Fig. 4b) in cross-shore and longshore currents, and water level, corresponding approximately to the mean incident wave periods with T_{zo} of 8.7 s. However, on day 2, spectral density was more spread out across all swell frequencies (Fig. 4b, d, f). There was a clear correspondence between cross-shore current spectral patterns and water level (e.g., Fig. 4a cf. 4e), and no strong correlation between longshore currents and water level (e.g., Fig. 4c cf. 4e, and 4d cf. 4f).

3.2. Surf zone exchange

On both days, drifters rotated clockwise in a prominent surf zone eddy (Fig. 5), where the offshore-directed component of the eddy was in the rip channel seaward of ADV 1. However, there was a stark contrast in drifter behavior between days in terms of surf zone exits and retention rates (Fig. 6). On day 1, during moderate wave conditions, the rate of surf zone exchange was high, with 71% of drifters (per rip entry) exiting the surf zone beyond the breaking waves (Fig. 5a and 6a). On day 2, during high energy waves, surf zone retention was high, with most drifters circulating around the surf zone eddy, and remaining inside the surf zone (Fig. 5b and 6b). On day 2, only one drifter exited the surf zone (exit rate = 6%). The higher exit rate on day 1 was associated with lower Γ (Fig. 5c), compared to on day 2 when most drifters were retained within the surf zone, and Γ was generally higher, particularly around the landward and seaward edges of the surf zone eddy (Fig. 5d). Vorticity was strongly positive ($\Gamma > 0.1$ m s^{-1}, anticlockwise) in a band across the center of the eddy, and strongly negative ($\Gamma < 0.1$ m s^{-1}, clockwise) in bands around the ends that were constricted by the shore and the inner bar. Once drifters have exited beyond the inner bar, Γ was generally ~zero, indicating that once drifters have exited the eddy, currents are no longer rotational (Fig. 5c, d).

3.3. Lagrangian pulsations

Pulsations in drifter velocity were O(~0.5–2 ms^{-1}). On day 1, during the moderate wave conditions (H_{so} = 1.4 m), pulsing was intermittent and occurred in bursts lasting 5–10 min, interspersed with periods of relatively constant, and lower velocities of < 0.5 ms^{-1} (Fig. 7a). On day 2, during the higher wave conditions (H_{so} = 1.9 m), current velocities were constantly pulsing throughout the measurements (Fig. 7b). While rip current velocities measured with drifters cannot be directly compared to the ADV measurements (which were shoreward and alongshore of the rip, see Fig. 1c), visual observations clearly showed that when drifters were deployed at the base of the rip channel, they were very quickly swept alongshore and offshore.

3.4. Role of wave breaking over the outer bar

Waves break when water depth is sufficiently shallow relative to wave height, where breaking wave height is classically defined as 0.78 of the water depth (e.g., Masselink et al., 2011). Throughout the drifter deployments, the occurrence of wave breaking over the inner and outer bars was turned on and off (Fig. 8a and c), and was strongly modulated by both tide and wave height. In the early morning on day 1, wave breaking occurred over the inner bar from low tide, at least up to mid-tide (Fig. 8a). The drifter deployments took place approaching high tide, at which time wave breaking did not occur over the inner bar (Fig. 8a). On the outer bar, wave breaking moved further inshore as water level increased (Fig. 8b), and wave similarly ceased approaching high tide (Fig. 8c). The camera outage makes it difficult to assess wave breaking on day 2, however it appears that there was a similar process of wave breaking over the inner and outer bars switching off with the rising tide.

4. Discussion

The aim of this study was to investigate surf zone exchange on a double barred beach, and the role of wave breaking on rip current dynamics. The exit rate from the surf zone to inner shelf decreased dramatically with increased wave breaking over the outer bar, from 71% on day 1 to 6% on day 2 (Fig. 6). This exit rate appears to be driven by the balance between: (1) wave breaking over the inner and outer bars, which determines if water parcels can 'escape' the surf zone eddy and exit beyond the breakers; and (2) pulsing of currents within the surf zone. Lagrangian measurements showed intermittent rip current pulsing on day 1, when incident wave energy was moderate (H_{so} = 1.4 m), and constant pulsing on day 2, when incident wave energy was 36% higher (H_{so} = 1.9 m). Thus, increased pulsing under high wave conditions does not necessarily increase surf zone exits. This is consistent with recent studies showing that low rip flow speeds under lower wave conditions can increase surf zone exits (Castelle et al., 2014b; Scott et al., 2014) (although they did not look at the relationship between pulsing and exits specifically).

Previous studies have linked the occurrence of surf zone exits to pulsations in rip current velocity at infragravity (~25–300 s)

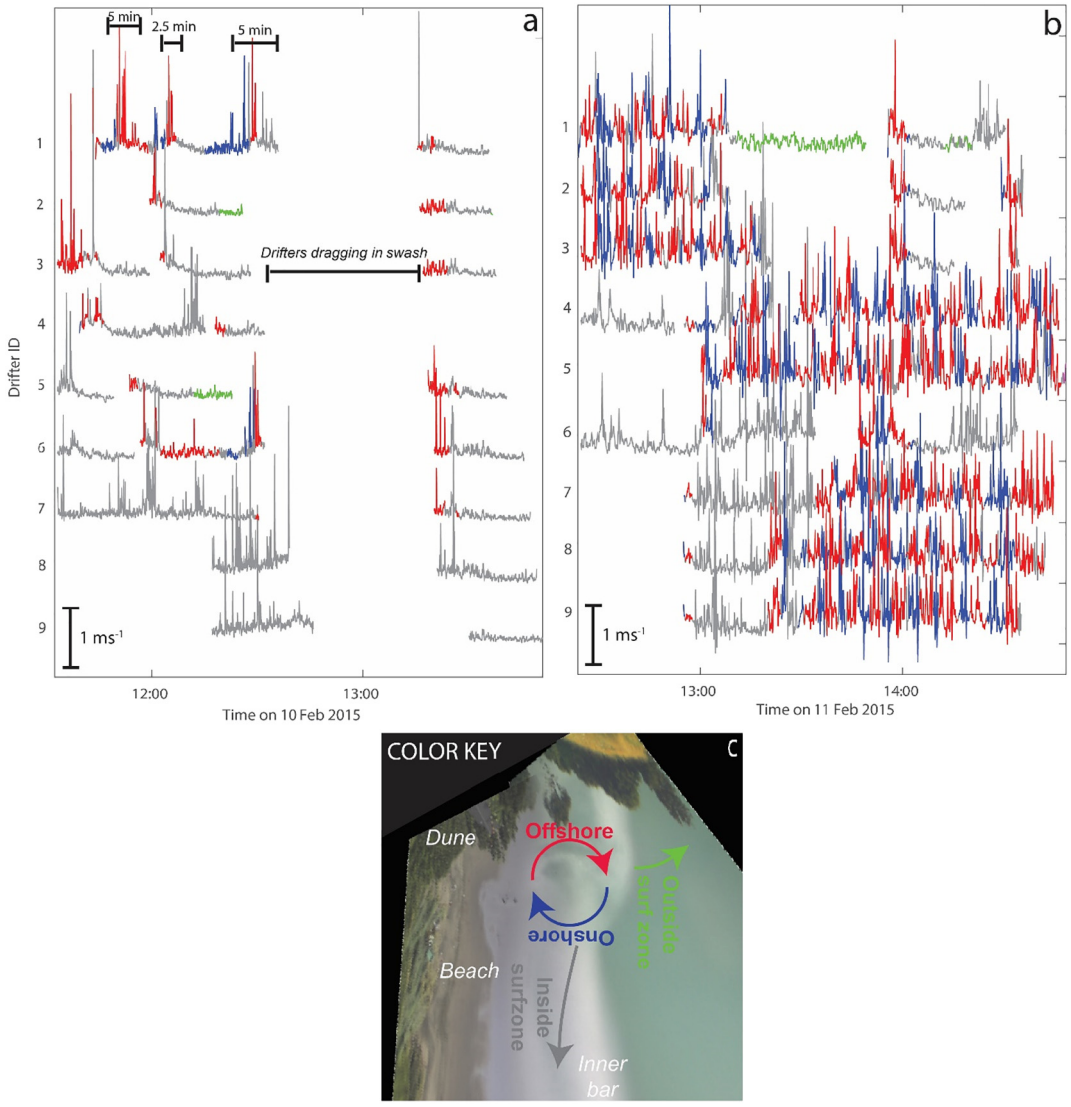

Fig. 7. (a) and (b) show filtered GPS drifter velocities. Drifter velocities are color coded by location/behavior, shown in the example timex image from 10/02/2016 at 11:59 in (c). Color key is an example timex image from 10/02/2015 at 17:00 and indicates (1) offshore- (red) and (2) onshore-directed (blue) flow in the rip current circulation cell; (3) elsewhere inside the surf zone (grey); and (4) offshore (seaward of the surf zone, green). Low tide on each day was at 11 am and 11:45 am. The gap in day 1 is a result of the quality control process, when redeployed drifters were largely dragging on the bottom and were not successfully transported into the surf zone eddy. (For interpretation of the references to color in this figure legend, the reader is referred to the web version of this article.)

(MacMahan et al., 2004a; Spydell and Feddersen, 2009; Reniers et al., 2010; Feddersen, 2014) and VLF frequencies (MacMahan et al., 2004b; Reniers et al., 2007, 2010; Feddersen et al., 2011; Castelle et al., 2013, 2014b; Houser et al., 2013; Brown et al., 2015). Although the Eulerian measurement locations did not coincide with the drifters and direct comparisons of current speeds could not be made, the ADV spectra also showed dominant infragravity energy when pulsations were also dominant. The mechanisms of the pulsations are outside the scope of this study, however, it is clear that more constant rip current pulsing occurs under higher wave energy, although it does not appear that this increases the surf zone exit rate, probably due to the balance with wave breaking on the outer bar, discussed below. Spatially, the pulsations occur when the drifters were caught in the main eddy (Fig. 5), but not when drifters exited the surfzone (see green in Fig. 7), thus the pulsations are associated with water circulating through the eddy. Spectra from the ADVs shows that infragravity spectral density in cross-shore currents was an order of magnitude higher on day 2 compared to day 1 (Fig. 4a, b), in accordance with the well-known relationship between offshore wave height and infragravity wave energy in the nearshore (e.g., Guza and Thornton, 1982; Ruessink et al., 1998). Furthermore, at the study site Ngarunui beach, (Guedes et al., 2013) showed that at the predominantly dissipative Ngarunui Beach, most infragravity forcing came from outside of the surf zone rather than due to generation in the surf zone such as by bore-bore capture of sea swell waves (e.g, Mase, 1995).

Previous studies suggest that rip flow generally remains within the surf zone due to eddies and Γ (MacMahan et al., 2010; Reniers et al., 2010; Castelle et al., 2010a). While the offshore-directed part of the surf zone eddy in this study was in the channel rip current, this rip was ~300 m away from a prominent headland, thus there could be some lee-side circulation effects due to wave shadowing (Gourlay, 1974; McCarroll et al., 2014; Pattiaratchi et al., 2009). The current study shows that the highest surf zone exit rate occurred when there was no wave breaking over the inner and outer bars on day 1 (Fig. 8a and c). Conversely, larger waves and hence increased breaking over both bars encouraged retention, as supported by observations elsewhere (Austin et al., 2013; Houser et al., 2013) This process is similar to a recent concept developed for single-barred beaches, of 'open rips' when there is no wave breaking across the seaward end of a rip channel, and 'closed rips' when wave breaking occurs across the seaward end of a rip

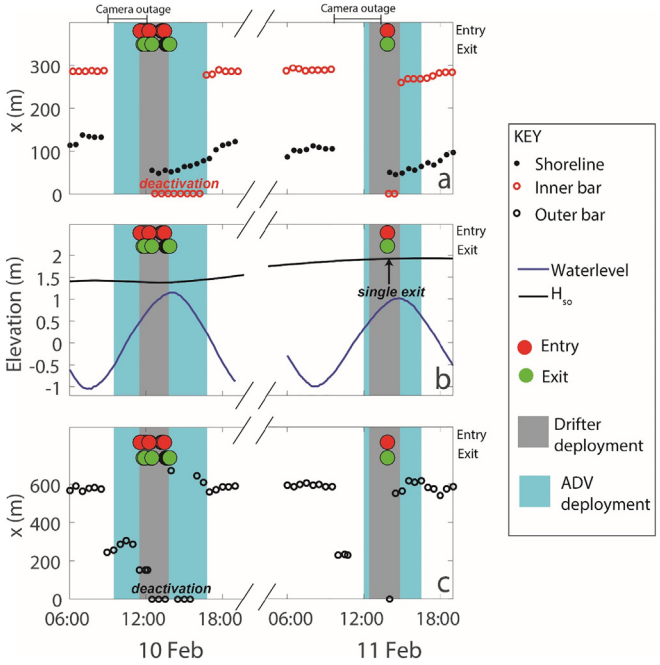

Fig. 8. Digitizations of the initialization of wave breaking on the: (a) inner bar (with shoreline also shown for reference); and (c) outer bar. (b) shows tidal elevation at the times the images were captured and H_{so}. Red and green dots indicate times when drifters entered and exited the surf zone respectively, and periods of camera outage are indicated. (For interpretation of the references to color in this figure legend, the reader is referred to the web version of this article.)

channel (Pitman et al., 2016). Rip closure at Ngarunui is inferred from the occurrence of breaking over the inner bar (Fig. 8a). This closure increased the rotational component of surf zone currents (as evidenced by Γ in Fig. 5c and d), in accordance with a 43% increase in Γ for closed compared to open rips at Perranporth Beach, U.K. (Pitman et al., 2016), and Santa Rosa Island, Florida, U.SA., where Houser et al. (2013) found increased Γ when the extent of wave breaking increased. Pitman et al. (2016) also found that in closed rips, drifter exits rates were < 25% compared to up to 91% for open rips, consistent with the exit rate of 6% for the closed rip and 71% for the open rip at Ngarunui. At Ngarunui, Γ was highest around the outside of the eddy, i.e., where the currents are constricted by the shore and outer bar and forced to rotate, rather than the center of the eddy as found for predominantly open rips in previous studies (e.g., McCarroll et al., 2014). Previous studies have shown the highest Γ at the center of the eddy (Castelle et al., 2010a; MacMahan et al., 2010; McCarroll et al., 2014); for these studies the effect of breaking across the seaward end of the channel was not explicitly reported, however it appears that there was a mix of open and closed rips.

While further investigation is required, the two days of Lagrangian measurements at Ngarunui suggest that there may be two different mechanisms responsible for exits from the surf zone, depending on wave breaking conditions across the outer bar (Fig. 9). On day 1, there was no wave breaking over the outer bar, and therefore no incident wave bores driving shoreward currents towards the inner bar, allowing water parcels (and drifters) to freely exit the surf zone (Fig. 9a). In contrast, on day 2, wave breaking over the outer bar means that now wave bores were driving shoreward return currents, pushing against the vortical currents of the surf zone eddy (Fig. 9b). In this situation, exits from the surf zone may only occur when a vortex is shed off the surf zone eddy (Castelle et al., 2010a), which have been described as filament-like Lagrangian Coherent Structures (LCS; Reniers et al., 2010; Castelle et al., 2013). Only a single LCS was observed at Ngarunui, and accounted for the single drifter exit observed on day 2 (Fig. 5b).

In summary, the interaction of surf zone bathymetry (i.e., sand bars and channels) with incident wave conditions appears to be a key driver of rip current circulation, in particular, of whether currents circulation in eddies within the surf zone, or exit beyond the outer bar. Rip current circulation patterns and exit rates have important implications for rip current hazards. Pitman et al. (2016) showed that at Perranporth, open rips were twice as dangerous to beach users in terms of requiring rescue by lifeguards. Further research is required to determine how such information could be used to reduce rip current hazards, such as which escape strategy to use (Miloshis and Stephenson, 2011; McCarroll et al., 2013; Castelle et al., 2016a, 2016b). In addition, there have been very few studies on the influence of outer bars on surf zone retention, which may have important implications for surf zone sediment transport and exchange (Orzech et al., 2011; Thorpe et al., 2013).

5. Conclusions

This study investigated rip current circulation and surf zone exchange at the high energy, double barred Ngarunui Beach in New Zealand. A key focus was on the role of wave breaking over the inner and outer bars on surf zone circulation and retention. Over the 2 days

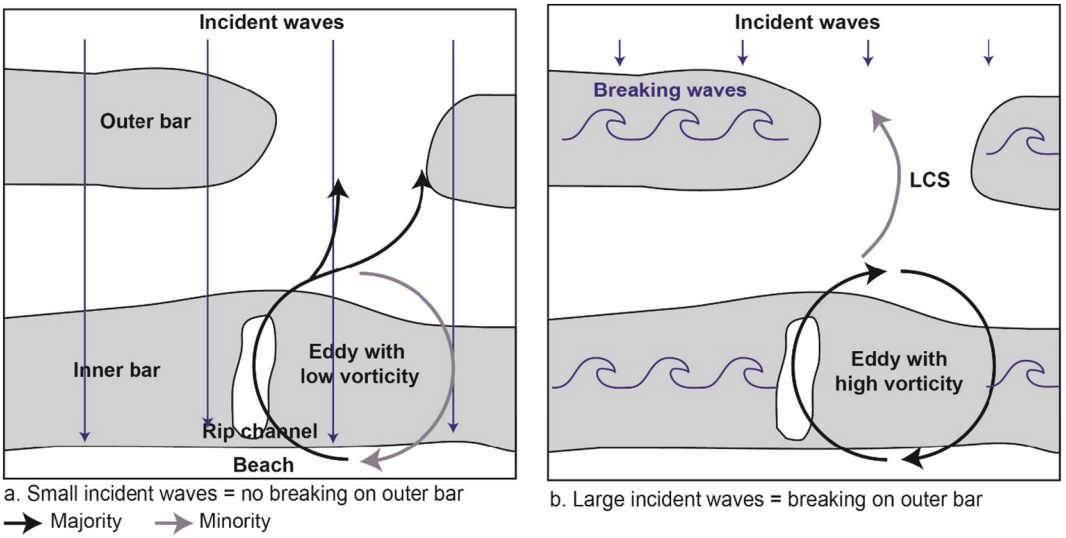

Fig. 9. Conceptual model of the two mechanisms for exits from eddies in the surf zone to beyond the breakers; during periods of (a) significant wave breaking over the outer bar; and (b) little or no wave breaking over the outer bar. LCS is Lagrangian Coherent Structure as defined by Reniers et al. (2010).

measured, there was a clockwise eddy in the surf zone, for which the seaward-heading portion formed a rip current in a well-defined channel rip incised into the inner bar. Exit rate (measured with GPS drifters) from the surf zone to inner shelf decreased significantly with increased wave breaking over the outer bar: from 71% exits to 6% over the two days. This exit rate appears to be driven by the balance between wave breaking over the inner and outer bars; and pulsing of currents within the surf zone. Under higher wave conditions, there were stronger pulsations in surf zone currents, which could lead to more surf zone exits. However, higher wave conditions caused wave breaking over the outer bar. This breaking increases vorticity around the outside of the surf zone eddy, which increase surf zone retention. This is in contrast to previous studies which found that vorticity is highest at the center of surf zone eddies. Under such conditions, drifter exits were rare, and occurred due to vortex shedding. During lower incident wave conditions, eddy vorticity is lower, and drifters can relatively freely exit the surf zone. This is one of the few studies that investigate surf zone circulation on high energy, double-barred beaches. Further investigation is required to investigate forcing mechanisms of the current pulsations (e.g., infragravity waves and VLF motions); and to determine how the balance of wave breaking and pulsations determines surf zone hazards on such beaches.

Acknowledgments and data

Thanks to the field volunteers (Mélanie Biausque, Carey Conn, Nicky Gallop, Steve Hunt, Jaco Labuschagne, Nicola Lovett, Chris Morcom, Julia Mullarney, Renaud Panier and Emily Woodhouse); the Raglan Coast Guard for their jetski (Ed Aktin and Sebastian Boulay); the Raglan Surf Life Saving Club; Brice Blossier for building and testing the drifters; Waikato Regional Council (Bronwen Gibberd) and NIWA (George Payne and Michael Ellis) for the Cam-Era video system; Richard Gorman (NIWA) for offshore model wave data; and the Institute of Marine Engineering, Science & Technology (IMarEST) Laurie Prandolini Fellowship for funding the field work. RR is supported by the AXA Research fund and the Deltares Strategic Research Programme 'Coastal and Offshore Engineering'. KRB was supported by MBIE contract UOWX1502. Thank you to Falk Feddersen for comments on an earlier version of this paper, and the two reviewers and editor for their constructive reviews. Data supporting the conclusions is located in the figures in this paper, and can also be requested from SLG.

References

Aagaard, T., Greenwood, B., Nielsen, J., 1997. Mean currents and sediment transport in a rip channel. Mar. Geol. 140 (1–2), 25–45. https://doi.org/10.1016/S0025-3227(97)00025-X.

Austin, M., Scott, T., Brown, J., Brown, J., MacMahan, J., Masselink, G., Russell, P., 2010. Temporal observations of rip current circulation on a macro-tidal beach. Cont. Shelf Res. 30 (9), 1149–1165. https://doi.org/10.1016/j.csr.2010.03.005.

Austin, M.J., Scott, T.M., Russell, P.E., Masselink, G., 2013. Rip current prediction: development, validation, and evaluation of an operational tool. J. Coast. Res. 29 (2), 283–300. https://doi.org/10.2112/JCOASTRES-D-12-00093.1.

Bierens, J.J.L.M. (Ed.), 2006. Handbook on Drowning: Prevention, Rescue, Treatment. Springer, Berlin.

Bowen, A., Inman, D., Simmons, V., 1968. Wave "set-down" and "set-up". J. Geophys. Res. 73 (8), 2569–2577. https://doi.org/10.1029/JB073i008p02569.

Brander, R.W., Macmahan, J.H., 2011. Future challenges for rip current research and education. In: Leatherman, S.P., Fletemeyer, J. (Eds.), Rip Currents: Beach Safety, Physical Oceanography and Wave Modelling. CRC Press, Boca Raton, pp. 1–29.

Brander, R.W., Short, A.D., 2000. Morphodynamics of a large-scale rip current system at Muriwai Beach, New Zealand. Mar. Geol. 165 (1–4), 27–39. https://doi.org/10.1016/S0025-3227(00)00004-9.

Brown, J., MacMahan, J., Reniers, A., Thornton, E., 2009. Surf zone diffusivity on a rip-channeled beach. J. Geophys. Res. Oceans 114, C11015. https://doi.org/10.1029/2008JC005158.

Brown, J.A., MacMahan, J.H., Reniers, A.J.H.M., Thornton, E.B., 2015. Field observations of surf zone-inner shelf exchange on a rip-channeled beach. J. Phys. Oceanogr. 45 (9), 2339–2355. https://doi.org/10.1175/JPO-D-14-0118.1.

Castelle, B., Coco, G., 2012. The morphodynamics of rip channels on embayed beaches. Cont. Shelf Res. 43, 10–23. https://doi.org/10.1016/j.csr.2012.04.010.

Castelle, B., Michallet, H., Marieu, V., Leckler, F., Dubardier, B., Lambert, A., Berni, C., Bonneton, P., Barthélemy, E., Bouchette, F., 2010a. Laboratory experiment on rip current circulations over a moveable bed: Drifter measurements. J. Geophys. Res. Oceans 115, C12008. https://doi.org/10.1029/2010JC006343.

Castelle, B., Ruessink, B.G., Bonneton, P., Marieu, V., Bruneau, N., Price, T.D., 2010b. Coupling mechanisms in double sandbar systems. Part 1: patterns and physical explanation. Earth Surf. Process. Landf. 35 (4), 476–486. https://doi.org/10.1002/esp.1929.

Castelle, B., Ruessink, B.G., Bonneton, P., Marieu, V., Bruneau, N., Price, T.D., 2010c. Coupling mechanisms in double sandbar systems. Part 2: impact on alongshore variability of inner-bar rip channels. Earth Surf. Process. Landf. 35 (7), 771–781. https://doi.org/10.1002/esp.1949.

Castelle, B., Reniers, A., MacMahan, J., 2013. Numerical modelling of surfzone retention in rip current systems: on the impact of the surfzone sandbar morphology. In: Proceedings of Coastal Dynamics 2013, Archachon, France.

Castelle, B., Almar, R., Dorel, M., Lefebvre, J.P., Senechal, N., Anthony, E.J., Laibi, R., Chuchla, R., du Penhoat, Y., 2014a. Rip currents and circulation on a high-energy low-tide-terraced beach (Grand Popo, Benin, West Africa). J. Coast. Res. SI70, 633–638. https://doi.org/10.2112/SI70-107.1.

Castelle, B., Reniers, A., MacMahan, J., 2014b. Bathymetric control of surf zone retention on a rip-channelled beach. Ocean Dyn. 64 (8), 1221–1231. https://doi.org/10.1007/s10236-014-0747-0.

Castelle, B., McCarroll, R.J., Brander, R.W., Scott, T., Dubarbier, B., 2016a. Modelling the alongshore variability of optimum rip current escape strategies on a multiple rip-channelled beach. Nat. Hazards 81 (1), 663–686. https://doi.org/10.1007/s11069-015-2101-3.

Castelle, B., Scott, T., Brander, R.W., McCaroll, R.J., 2016b. Rip current types, circulation and hazard. Earth Sci. Rev. 163, 1–21. https://doi.org/10.1016/j.earscirev.2016.09.008.

Dalrymple, R.A., MacMahan, J.H., Reniers, A.J.H.M., Nelko, V., 2011. Rip currents. Annu. Rev. Fluid Mech. 43 (1), 551–581. https://doi.org/10.1146/annurev-fluid-122109-160733.

Defeo, O., McLachlan, A., 2005. Patterns, processes and regulatory mechanisms in sandy beach macrofauna: a multi-scale analysis. Mar. Ecol. Prog. Ser. 295, 1–20. https://doi.org/10.3354/meps295001.

Feddersen, F., 2014. The generation of surfzone eddies in a strong alongshore current. J. Phys. Oceanogr. 44, 600–617. https://doi.org/10.1175/JPO-D-13-051.1.

Feddersen, F., Clark, D.B., Guza, R.T., 2011. Modeling surf zone tracer plumes: 1. Waves, mean currents, and low-frequency eddies. J. Geophys. Res. Oceans 116, C11027. https://doi.org/10.1029/2011JC007210.

Feng, Z., Reniers, A., Haus, B.K., Solo-Gabriele, H.M., 2013. Modeling sediment-related enterococci loading, transport and inactivation at an embayed nonpoint source beach. Water Resour. Res. 49 (2), 693–712. https://doi.org/10.1029/2012WR012432.

Fujimura, A.G., Reniers, A.J.H.M., Paris, C.B., Shanks, A.L., MacMahan, J.H., Morgan, S.G., 2014. Numerical simulations of larval transport into a rip-channeled surf zone. Limnol. Oceanogr. 59 (4), 1434–1447. https://doi.org/10.4319/lo.2014.59.4.1434.

Gallop, S.L., Bryan, K.R., Coco, Giovanni, 2009. Video observations of rip currents on an embayed beach. J. Coast. Res. SI56, 49–53.

Gallop, S.L., Bryan, K.R., Coco, Giovanni, Stephens, S.A., 2011. Storm-driven changes in rip channel patterns on an embayed beach. Geomorphology 127 (3–4), 179–188. https://doi.org/10.1016/j.geomorph.2010.12.014.

Gallop, S.L., Bryan, K.R., Pitman, S., Ranasinghe, R., Sandwell, D., 2015. Rip current observations on a low-sloping dissipative beach. In: Proceedings of the Australasian Coasts and Ports Conference, Auckland, New Zealand.

Gallop, S.L., Bryan, K.R., Pitman, S.J., Ranasinghe, R., Sandwell, D., 2016. Pulsations in surf zone currents on a high energy mesotidal beach in New Zealand, Proceedings of the International Coastal Symposium, Sydney, Australia. J. Coast. Res. SI75, 912–916.

Gorman, R.M., Bryan, K.R., Laing, A.K., 2003. Wave hindcast for the New Zealand region: Nearshore validation and coastal wave climate. N. Z. J. Mar. Freshw. Res. 37 (3), 567–588. https://doi.org/10.1080/00288330.2003.9517190.

Gourlay, M.R., 1974. Wave set-up and wave generated currents in the lee of a breakwater or headland. In: In: Coastal Engineering 1974: Proceedings of the Fourteenth International Conference. American Society of Civil Engineers, New York, pp. 1976–1995.

Guedes, R.M.C., Bryan, K.R., Coco, G., 2013. Observations of wave energy fluxes and swash motions on a low-sloping, dissipative beach. J. Geophys. Res. Oceans 118 (7), 3651–3669. https://doi.org/10.1002/jgrc.20267.

Guza, R.T., Thornton, E.B., 1982. Swash oscillations on a natural beach. J. Geophys. Res. Oceans 87, 483–491. https://doi.org/10.1029/JC087iC01p00483.

Hally-Rosendahl, K., Feddersen, F., Clark, D.B., Guza, R.T., 2015. Surfzone to inner-shelf exchange estimated from dye tracer balances. J. Geophys. Res. Oceans 120 (9), 6289–6308. https://doi.org/10.1002/2015JC010844.

Harrison, S.R., 2015. Morphodynamics of Ebb-Tidal Deltas. Ph.D. Thesis. The University of Waikato, Hamilton, New Zealand.

Harrison, S.R., Hunt, S., 2014. Whaingaroa harbour, New Zealand. Hydrographic chart. In: Distributed by the University of Waikato and Waikato Regional Council at NZCS 2014, Raglan.

Harrison, S.R., Bryan, K.R., Mullarney, J.C., 2017. Observations of morphological change at an ebb-tidal delta. Mar. Geol. 385, 131–145. https://doi.org/10.1016/j.margeo.2016.12.010.

Holman, R.A., Symonds, G., Thornton, E.B., Ranasinghe, R., 2006. Rip spacing and persistence on an embayed beach. J. Geophys. Res. Oceans 111, C01006. https://doi.org/10.1029/2005JC002965.

Houser, C., Arnott, R., Ulzhöfer, S., Barnett, G., 2013. Nearshore circulation over transverse bar and rip morphology with oblique wave forcing. Earth Surf. Process. Landf.

38 (11), 1269–1279. https://doi.org/10.1002/esp.3413.
Huisman, C.E., Bryan, K.R., Coco, G., Ruessink, B.G., 2011. Use of video imagery to analyse groundwater and shoreline dynamics on a dissipative beach. Cont. Shelf Res. 31 (16), 1728–1738. https://doi.org/10.1016/j.csr.2011.07.013.
Johnson, D., Pattiaratchi, C., 2004. Transient rip currents and nearshore circulation on a swell-dominated beach. J. Geophys. Res. Oceans 109, C02026. https://doi.org/10.1029/2003JC001798.
Johnson, D., Pattiaratchi, C., 2006. Boussinesq modeling of transient rip currents. Coast. Eng. 53 (5–6), 419–439. https://doi.org/10.1016/j.coastaleng.2005.11.005.
Kumar, N., Feddersen, F., 2016a. The effect of Stokes drift and transient rip currents on the inner-shelf, part 1: no stratification. J. Phys. Oceanogr. 47, 227–241. https://doi.org/10.1175/JPO-D-16-0076.1.
Kumar, N., Feddersen, F., 2016b. The effect of Stokes drift and transient rip currents on the inner-shelf, part 2: with stratification. J. Phys. Oceanogr. 47, 243–260. https://doi.org/10.1175/JPO-D-16-0077.1.
Long, J.W., Özkan-Haller, H.T., 2005. Offshore controls on nearshore rip currents. J. Geophys. Res. Oceans 110, C12007. https://doi.org/10.1029/2005JC003018.
Long, J.W., Özkan-Haller, H.T., 2016. Forcing and variability of nonstationary rip currents. J. Geophys. Res. Oceans 121, 520–539. https://doi.org/10.1002/2015JC010990.
Loureiro, C., Ferreira, Ó., Cooper, J.A.G., 2012. Extreme erosion on high-energy embayed beaches: influence of megarips and storm grouping. Geomorphology 139–140, 155–171. https://doi.org/10.1016/j.geomorph.2011.10.013.
MacMahan, J.H., Reniers, A.J.H.M., Thornton, E.B., Stanton, T.P., 2004a. Infragravity rip current pulsations. J. Geophys. Res. Oceans 109, C01033. https://doi.org/10.1029/2003JC002068.
MacMahan, J.H., Reniers, A.J.H.M., Thornton, E.B., Stanton, T.P., 2004b. Surf zone eddies coupled with rip current morphology. J. Geophys. Res. Oceans 109, C07004. https://doi.org/10.1029/2003JC002083.
MacMahan, J., Brown, J., Thornton, E., 2009. Low-cost handheld global positioning system for measuring surf-zone currents. J. Coast. Res. 25 (3), 744–754. https://doi.org/10.2112/08-1000.1.
MacMahan, J., Brown, J., Brown, J., Thornton, E., Reniers, A., Stanton, T., Henriquez, M., Gallager, E., Morrison, J., Austin, M.J., Scott, T.M., Senechal, N., 2010. Mean Lagrangian flow behaviour on an open coast rip-channeled beach: a new perspective. Mar. Geol. 268 (1–4), 1–15. https://doi.org/10.1016/j.margeo.2009.09.011.
Mase, H., 1995. Frequency down-shift of swash oscillations compared to incident waves. J. Hydraul. Res. 33, 397–411. https://doi.org/10.1080/00221689509498580.
Masselink, G., Short, A.D., 1993. The effect of tide range on beach morphodynamics and morphology: a conceptual beach model. J. Coast. Res. 9 (3), 785–800.
Masselink, G., Hughes, M.G., Knight, J., 2011. Introduction to Coastal Processes and Geomorphology. Hodder Education, London.
McCarroll, R.J., Brander, R.W., MacMahan, J.H., Turner, I.L., Reniers, A.J.H.M., Brown, J.A., Bradstreet, A., 2013. Assessing the effectiveness of rip current swimmer escape strategies, Shelly Beach, NSW, Australia. J. Coast. Res. SI65, 784–789.
McCarroll, R.J., Brander, R.W., Turner, I.L., Power, H.E., Mortlock, T.R., 2014. Lagrangian observations of circulation on an embayed beach with headland rip currents. Mar. Geol. 355, 173–188. https://doi.org/10.1016/j.margeo.2014.05.020.
Miloshis, M., Stephenson, W.J., 2011. Rip current escape strategies: lessons for swimmer and coastal rescue authorities. Nat. Hazards 59 (2), 823–832. https://doi.org/10.1007/s11069-011-9798-4.
Molinari, R., Kirwan Jr., A.D., 1975. Calculations of differential kinematic properties from lagrangian observations in the Western Caribbean Sea. J. Phys. Oceanogr. 5, 483–491. https://doi.org/10.1175/1520-0485(1975)005<0483:CODKPF>2.0.CO;2.
Orzech, M.D., Reniers, A.J.H.M., Thornton, E.B., MacMahan, J.H., 2011. Megacusps on rip channel bathymetry: observations and modelling. Coast. Eng. 58 (9), 890–907. https://doi.org/10.1016/j.coastaleng.2011.05.001.
Özkan-Haller, H.T., Kirby, J.T., 1999. Nonlinear evolution of shear instabilities of the longshore current: a comparison of observations and computations. J. Geophys. Res. Oceans 104, 25953–25984. https://doi.org/10.1029/1999JC900104.
Pattiaratchi, C., Olsson, D., Hetzel, Y., Lowe, R., 2009. Wave-driven circulation patterns in the lee of groynes. Cont. Shelf Res. 29 (16), 1961–1974. https://doi.org/10.1016/j.csr.2009.04.011.
Pitman, S., Gallop, S.L., Haigh, I.D., Masselink, G., Ranasinghe, R., 2016. Wave breaking patterns control rip current flow regimes and surfzone retention. Mar. Geol. 382, 176–190. https://doi.org/10.1016/j.margeo.2016.10.016.
Price, T.D., Ruessink, B.G., Castelle, B., 2014. Morphological coupling in multiple sandbar systems - a review. Earth Surf. Dyn. 2 (1), 309–321. https://doi.org/10.5194/esurf-2-309-2014.
Reniers, A.J.H.M., MacMahan, J.H., Thornton, E.B., Stanton, T.P., 2007. Modeling of very low frequency motions during RIPEX. J. Geophys. Res. Oceans 112, C07013. https://doi.org/10.1029/2005JC003122.
Reniers, A.J.H.M., MacMahan, J.H., Thornton, E.B., Stanton, T.P., Henriquez, M., Brown, J.W., Brown, J.A., Gallagher, E.L., 2009. Surfzone retention on a rip-channeled beach. J. Geophys. Res. Oceans 114, C10010. https://doi.org/10.1029/2008JC005153.
Reniers, A.J.H.M., MacMahan, J.H., Beron-Vera, F.J., Olascoaga, M.J., 2010. Rip-current pulses tied to Lagrangian coherent structures. Geophys. Res. Lett. 37 (5), L05605. https://doi.org/10.1029/2009GL041443.
Ruessink, B.G., Kleinhansm, M.G., vanden Beukel, P.G.L., 1998. Observations of swash under highly dissipative conditions. J. Geophys. Res. Oceans 103, 3111–3118. https://doi.org/10.1029/97JC02791.
Schmidt, W.E., Woodward, B.T., Millikan, K.S., Guza, R.T., Raubenheimer, B., Elgar, S., 2003. A GPS-tracked surf zone drifter. J. Atmos. Ocean. Technol. 20, 1069–1075. https://doi.org/10.1175/1460.1.
Scott, T., Masselink, G., Austin, M.J., Russell, P., 2014. Controls on macrotidal rip current circulation and hazard. Geomorphology 214, 198–215. https://doi.org/10.1016/j.geomorph.2014.02.005.
Scott, T., Austin, M., Masselink, G., Russell, P., 2016. Dynamics of rip currents associated with groynes — field measurements, modelling and implications for beach safety. Coast. Eng. 107, 53–69. https://doi.org/10.1016/j.coastaleng.2015.09.013.
Sherwood, A.M., Nelson, C.S., 1979. Surficial sediments of Raglan Harbour. N. Z. J. Mar. Freshw. Res. 13 (4), 475–496. https://doi.org/10.1080/00288330.1979.9515825.
Short, A.D., 1985. Rip-current type, spacing and persistence, Narrabeen Beach, Australia. Mar. Geol. 65 (1–2), 47–71. https://doi.org/10.1016/0025-3227(85)90046-5.
Short, A.D., Aagaard, T., 1993. Single and multi-bar beach change models. J. Coast. Res. SI15, 141–157.
Simarro, G., Bryan, K.R., Guedes, R.M.C., Sancho, A., Guillen, J., Coco, G., 2015. On the use of variance images for runup and shoreline detection. Coast. Eng. 99, 136–147. https://doi.org/10.1016/j.coastaleng.2015.03.002.
Smith, J.A., Largier, J.L., 1995. Observations of nearshore circulation: rip currents. J. Geophys. Res. Oceans 100 (C6), 10967–10975. https://doi.org/10.1029/95JC00751.
Sonu, C.J., 1972. Field observation of nearshore circulation and meandering currents. J. Geophys. Res. 77 (18), 3232–3247. https://doi.org/10.1029/JC077i018p03232.
Spydell, M.S., 2016. The suppression of surfzone cross-shore mixing by alongshore currents. Geophys. Res. Lett. 43 (18), 9781–9790. https://doi.org/10.1002/2016GL070626.
Spydell, M.S., Feddersen, F., 2009. Lagrangian drifter dispersion in the surf zone: directionally spread, normally incident waves. J. Phys. Oceanogr. 39, 809–830. https://doi.org/10.1175/2008JPO3892.1.
Spydell, M.S., Feddersen, F., 2012. A lagrangian model of surfzone drifter dispersion. J. Geophys. Res. Oceans 117, C03041. https://doi.org/10.1029/2011JC007701.
Spydell, M., Feddersen, F., Guza, R.T., Schmidt, W.E., 2007. Observing surf-zone dispersion with drifters. J. Phys. Oceanogr. 37, 2920–2939. https://doi.org/10.1175/2007JPO3580.1.
Spydell, M.S., Feddersen, F., Guza, R.T., 2009. Observations of drifter dispersion in the surfzone: the effect of sheared alongshore currents. J. Geophys. Res. Oceans 114, C07028. https://doi.org/10.1029/2009JC005328.
Spydell, M.S., Feddersen, F., Guza, R.T., MacMahan, J.H., 2014. Relating Lagrangian and Eulerian horizontal eddy statistics in the surfzone. J. Geophys. Res. Oceans 119 (2), 1022–1037. https://doi.org/10.1002/2013JC009415.
Suanda, S.H., Feddersen, F., 2015. A self-similar scaling for cross-shelf exchange driven by transient rip currents. Geophys. Res. Lett. 42 (13), 5247–5434. https://doi.org/10.1002/2015GL063944.
Talbot, M.M.B., Bate, G.C., 1987. Rip current characteristics and their role in the exchange of water and surf diatoms between the surf zone and nearshore. Estuar. Coast. Shelf Sci. 25 (6), 707–720. https://doi.org/10.1016/0272-7714(87)90017-5.
Thorpe, A., Miles, J., Masselink, G., Russell, P., Scott, T., Austin, M., 2013. Suspended sediment transport in rip currents on a macrotidal beach. J. Coast. Res. SI65, 1880–1885.
Van Enckevort, I.M.J., Ruessink, B.G., 2001. Effects of hydrodynamics and bathymetry on video estimates of nearshore sandbar position. J. Geophys. Res. Oceans 106 (C8), 16969–16979. https://doi.org/10.1029/1999JC000167.
Van Leeuwen, B.R., McCarroll, R.J., Brander, R.W., Turner, I.L., Power, H.E., Bradstreet, A.J., 2016. Examining rip current escape strategies in non-traditional beach morphologies. Nat. Hazards 81 (1), 145–165. https://doi.org/10.1007/s11069-015-2072-4.
Walters, R.A., Goring, D.G., Bell, R.G., 2001. Ocean tides around New Zealand. N. Z. J. Mar. Freshw. Res. 35 (3), 567–579. https://doi.org/10.1080/00288330.2001.9517023.